In Situ Studies of the Primary Immune Response to (4-hydroxy-3-nitrophenyl)acetyl. I. The Architecture and Dynamics of Responding Cell Populations

By Joshy Jacob,* Ramtin Kassir,‡ and Garnett Kelsoe*

*From the *Department of Microbiology and Immunology, University of Maryland School of Medicine, Baltimore, Maryland 21201; and the ‡Department of Microbiology, University of Texas Medical Branch, Galveston, Texas 77550*

Summary

After primary immunization with an immunogenic conjugate of (4-hydroxy-3-nitrophenyl)acetyl, two anatomically and phenotypically distinct populations of antibody-forming cells arise in the spleen. As early as 2 d after immunization, foci of antigen-binding B cells are observed along the periphery of the periarteriolar lymphoid sheaths. These foci expand, occupying as much as 1% of the splenic volume by day 8 of the response. Later, foci grow smaller and are virtually absent from the spleen by day 14. A second responding population, germinal center B cells, appear on day 8–10 and persist at least until day 16 post-immunization. Individual foci and germinal centers represent discrete pauciclonal populations that apparently undergo somatic evolution in the course of the primary response. We suggest that foci may represent regions of predominantly interclonal competition for antigen among unmutated B cells, while germinal centers are sites of intraclonal clonal competition between mutated sister lymphocytes.

Before the selective action of antigens, the antibody repertoire of adult mice appears to be determined by a collection of stochastic processes. Probabilistic use and association of V, D, and J gene segments (1–9), the introduction of random junctional and N sequence diversity (10–12), and the independence of the *Igh*, -κ, and -λ loci (13) interact to produce a large and diverse collection of antigen-combining sites, or paratopes, that appears to be phenotypically neutral, i.e., unbiased for particular specificities (14–16). In contrast, the introduction of antigen activates deterministic processes that lead to nonrandom distributions of cells and molecules. Although simple in principle, antigen-driven proliferation and selection is a complex and poorly understood process. For example, given the current paradigm of antigen activation and clonal expansion, it is surprising that a large portion of induced Ig may not be specific for the immunogen (17, 18). Indeed, in some secondary responses the amount of unspecific Ig produced may exceed that of antigen-binding antibody (19). Or, while the kinds and frequency of B cells capable of responding to antigen have been determined in a variety of assays (20–23), those that actually do so in the spleen remains obscure. Our understanding of the immune response in vivo is limited, in part because of the common use of experimental and analytical methodologies based upon the use of dissociated immunocytes. Although such methods are expedient and powerful, e.g., the molecular genetic description of sets of related hybridomas, their nature limits study of potentially important cellular associations and interactions.

For these reasons, we have begun an investigation of the immune response to immunogenic conjugates of (4-hydroxy-3-nitrophenyl)acetyl (NP)[1] as it occurs within the spleen of C57BL/6 mice. The response to NP is genetically restricted; the majority of primary anti-NP antibodies are heteroclitic (24), bear the λ1 L chain (25, 26), possess a distinctive idiotype (25–27), and use the V186.2 segment of the V_HJ558 gene family to encode the H chain variable region (28). To characterize the cellular events that follow challenge with NP, we made serial, 6-μm-thick sections of spleens taken from mice immunized 2–16 d earlier. Antigen-induced clonal activation, proliferation, and differentiation were studied by the use of fluorochrome- or enzyme-coupled antibodies, antigen, and lectin, and digoxigenin-labeled DNA probes specific for the hallmarks of this response. These reagents, in combination with computer-aided reconstruction of the sectioned spleens, have allowed us to detail the architecture and clonal dynamics of an immune response.

Our studies reveal that initially, the antibody-producing cells of the primary response are clustered into discrete foci that originate from one to a few (≤3) precursor cells. Such foci arise in the periarteriolar lymphoid sheath (PALS) and near the terminal arteriolar branches, do not bind the lectin,

[1] *Abbreviations used in this paper:* 3-AEC, 3-amino-ethyl-carbozole; CG, chicken gamma globulin; GC, germinal centers; HRP, horseradish peroxidase; NIP, (4-hydroxy-5-iodo-3-nitrophenyl)acetyl; NP, (4-hydroxy-3-nitrophenyl)acetyl; PALS, periarteriolar lymphoid sheath; PNA, peanut agglutinin; S-AP, streptavidin-alkaline phosphatase; S-PE, streptavidin-PE.

 J. Exp. Med. © The Rockefeller University Press • 0022-1007/91/05/1165/11 $2.00
Volume 173 May 1991 1165–1175

peanut agglutinin (PNA), and are genetically isolated from one another, apparently evolving independently during the course of the response. A second, anatomically distinct population of antigen-induced B cells is observed in germinal centers (GC) that form 8 d after immunization and are readily identified by avid binding of PNA (29). During the time that foci and GC coexist within the immune spleen (days 8–12), no physical communication between the two populations is apparent. We have shown (unpublished results) that at least by day 16 post-immunization, individual GC represent mono- or oligoclonal populations of B cells that have undergone intraclonal diversification by somatic hypermutation and selection (30–34). Thus, it may be that the B cells responding within the PALS-associated foci and GC represent two distinct stages of clonal proliferation and competition in the primary response.

Materials and Methods

Animals. C57BL/6, BALB/c, and (C57BL/6 × BALB/c)F_1 mice (2–3 mo old) were purchased from Charles River Breeding Laboratories, Inc. (Wilmington, MA) or The Jackson Laboratory (Bar Harbor, ME), maintained, and bred locally. Mice were housed in microisolator cages, fed ad libitum, and maintained on a 12-h day/night cycle.

Antigens and Immunizations. The succinic anhydride ester of NP (Cambridge Research Biochemicals, Cambridge, UK) was reacted with chicken gamma globulin (CG) (Accurate Scientific, Westbury, NY) and precipitated in alum (NP-CG/alum). Groups of C57BL/6 and F_1 mice were immunized with a single intraperitoneal injection of 50 μg NP-CG/alum. Another group of C57BL/6 mice were immunized with in intraperitoneal injection of 50 μg of the antiidiotope mAb, Ac38, coupled to keyhole limpet hemocyanin (Ac38-KLH), and precipitated in alum as described by Tesch et al. (35). For controls, a number of C57BL/6 mice were immunized with 50 μg CG precipitated in alum (CG/alum).

Preparation of Spleen Sections. To establish the cellular dynamics of the splenic response, cohorts of immunized mice were killed at 2, 4, 6, 8, 10, 12, 14, or 16 d post-immunization, their spleens removed, and embedded in Tissue-Tek OCT compound (Fischer Scientific, Silver Spring, MD) by flash-freezing in 2-methyl butane (Aldrich Chemical Co., Milwaukee, WI) cooled with liquid N_2. Blocks of frozen tissue were stored at −70°C until sectioning. Spleens were cut on a cryostat (International Equipment Co., Needham Heights, MA) as 6-μm thick longitudinal sections and thaw mounted onto 0.05% poly-L-lysine (Sigma Chemical Co., St. Louis, MO) -coated slides. Sections were allowed to air dry for 10 min, fixed in ice-cold acetone (Fischer Scientific) for 10 min, air dried, and stored at −20°C until use. Spleens from mice immunized with Ac38-KLH/alum or CG/alum were processed identically.

Antibodies and Staining Reagents. Goat anti-mouse λ L chain antibody conjugated with FITC (anti-λ-FITC), horseradish peroxidase (HRP)-labeled goat anti-mouse λ L chain (anti-λ-HRP), biotinylated goat anti-rat Ig antibodies, streptavidin-PE (S-PE), and streptavidin-alkaline phosphatase (S-AP) were purchased from Southern Biotechnology Associates Inc. (Birmingham, AL). Anti-Thy-1.2 antibody and PNA-biotin were purchased from ICN Biomedicals Inc. (Costa Mesa, CA) and E-Y Laboratories (San Mateo, CA), respectively. The rat anti-mouse CD4 hybridoma line, GK1.5 (a gift from Dr. J. Cerny, University of Maryland School of Medicine), was expanded in culture and secreted antibody was purified by double precipitation in ammonium sulfate. The antiidiotypic mAbs Ac38 and Ac146 (27) were gifts of Dr. T. Imanishi-Kari (Tufts University, School of Medicine), and the anti-mouse λ_1 L chain antibody, Ls136 (36), and the antiallotype (anti-IgM^a) antibody, RS-3.1 (37), conjugated with FITC, were obtained from Dr. K. Rajewsky (University of Cologne). Hybridomas Ac38 and Ac146 were grown in culture, and their antibody products purified by ammonium sulfate precipitation followed by anion exchange chromatography on DEAE-sepharose. BSA was purchased from United States Biochemical Corp. (Cleveland, OH). The succinic anhydride ester of (4-hydroxy-5-iodo-3-nitrophenyl) acetyl (NIP) (Cambridge Research Biochemicals) was conjugated to BSA (NIP-BSA). NIP-BSA, Ac38, Ac146, Ls136, CG, and PNA were biotinylated with biotin-*N*-hydroxy succinamide (Vector Laboratories Inc., Burlingame, CA) using a protocol supplied by the manufacturer.

In Situ Immunofluorescence of Antigen-activated B Cells. Appropriate dilutions for staining reagents were ascertained by checkerboard titrations on cytocentrifuge preparations of the hybridoma B1-8 (36), which produces antibody that binds NP, bears the λ_1 L chain, and expresses the Ac38 and Ac146 idiotypes (27). For immunofluorescence, splenic sections were rehydrated in PBS, pH 7.4, blocked with PBS containing 3% BSA (PBS/BSA) for 30 min, incubated with NIP-BSA-biotin for 60 min, washed extensively in PBS/BSA, incubated with S-PE (4 μg/ml) for 45 min, washed in PBS/BSA, incubated with anti-λ-FITC (5 μg/ml) for 30 min, washed in PBS/BSA, and mounted in glycerol-PBS (1:1). All incubations were carried out at room temperature in a humid environment protected from light. Fluorescence was stabilized using a stabilizer provided by Amersham Corp. (Arlington Heights, IL). Staining with antiidiotypic antibodies and CG-biotin was done in an analogous manner. Adjacent spleen sections were stained with NIP-BSA-biotin and anti-λ-FITC in tandem, or with Ac38-biotin, Ac146-biotin, or CG-biotin in combination with anti-λ-FITC. Slides were examined with a Nikon Labphot fluorescence microscope and representative NP-reactive foci photographed using a Nikon N2000 camera. Examination of three adjacent serial sections permitted study of the distribution of paratopic and idiotopic specificities, within single λ^+ foci and GC.

Immunocytochemical Staining of Splenic Sections. Before immunocytochemical staining, spleen sections were rehydrated and blocked as described above. Sections were stained in tandem with anti-λ-HRP and anti-Thy-1.2-biotin or GK1.5. Bound GK1.5 antibody was detected using anti-rat Ig-biotin; bound biotinylated antibodies were then visualized using S-AP followed by enzymatic detection with 0.125, 0.25, and 0.25 mg/ml of naphthol-AS-MX phosphate (Sigma Chemical Co.), Fast Blue BB salt (Sigma Chemical Co.), and levamisole (Sigma Chemical Co.) in 0.1 M Tris-HCl, pH 8.5, respectively, as described (38). Endogenous peroxidase activity was blocked by a 10-min incubation in 3% H_2O_2 before staining. HRP-labeled antibodies were visualized using 1 mg/ml 3-aminoethyl-carbazole (3-AEC) (Sigma Chemical Co.) and 0.0015% H_2O_2 in 0.1 M sodium acetate buffer, pH 5.0, as described (38). Adjacent sections were similarly stained with PNA-biotin. Stained sections were washed in PBS and mounted (Crystal Mount; Biomeda Corp., Foster City, CA).

Three-dimensional Reconstruction of Splenic Architecture from Serial Sections. Serial spleen sections were stained with anti-Thy-1.2-biotin or PNA-biotin and anti-λ-HRP in tandem as described. Sections were photographed (×40), and the positions of PNA^+, T cell, and λ^+ colonies digitized using Jandel's digitizing tablet; computer-aided three-dimensional reconstructions of spleen were made from serial sections using three-dimensional reconstruction software, PC3D (Jandel Scientific, Corte Madera, CA). Volume measurements

of λ^+ foci and GC were obtained using the algorithm provided in the PC3D program.

DNA Probes. Plasmids p19.7-V4 (V186.2, DFL16.1, J_H2 [39]) and pABλ_1 ($V_{\lambda 1}$, $J_{\lambda 1}$, $C_{\lambda 1}$ [40]) were gifts from Drs. K. Rajewsky and A. L. M. Bothwell (Yale University), respectively. Competent HB101 cells were transformed with the plasmids using $CaCl_2$ and large-scale plasmid preparations made as described (41). After purification, plasmids were digested with appropriate restriction endonucleases. The 400-bp PstI-XbaI fragment of p19.7-V4 and the 400-bp PstI fragment of pABλ_1 were recovered from 0.8% agarose (Bethesda Research Laboratories, Gaithersburg, MD) gels using NA-45 anion exchange paper (Schleicher & Schuell, Inc., Keene, NH), eluted, precipitated with ethanol, and dried in a vacuum-centrifuge. The recovered λ1 insert was resuspended in sterile water and labeled with digoxigenin (dig)-UTP by random priming as directed by the manufacturer (Genius Kit; Boehringer Mannheim Biochemicals, Indianapolis, IN). That portion of the recovered p19.7-V4 insert containing the V186.2 sequence was labeled with dig using the PCR. Primers complementary to 20-bp regions at the 5′ and 3′ ends of the V186.2 gene segment (5′ TCT AGA ATT CAG GTC CAA CTG CAG CAG CC 3′ and 5′ GTC GAC GCG GCC GCA TAA TAG ACC GCA GAG TCC T 3′, respectively) were synthesized on a DNA synthesizer (380-A; Applied Biosystems, Inc., Foster City, CA). 5 ng of p19.7-V4 was amplified by PCR for 25 cycles in a 50-μl volume as follows: denaturation of template at 96°C for 1.4 min, and annealing and primer extension for 2 min at 70°C. The reaction mix comprised of 10 mM Tris-HCl (pH 8.3), 50 mM KCl, 4 mM $MgCl_2$, 0.01% gelatin (Sigma Chemical Co.), 100 μM dig-dNTP mix (Genius kit), 20 pmol primers, and 2.5 U Taq polymerase (Bethesda Research Laboratories). Two drops of mineral oil (Sigma Chemical Co.) were added to each tube to prevent evaporation. Probe concentration was determined by comparing intensities on an ethidium bromide–stained 1% agarose gel. Amplified DNA was used for hybridization without further purification. Dig-labeled probes were dried in a vacuum centrifuge, resuspended in sterile water, aliquoted, and stored at −20°C until use. Incorporation of dig-labeled nucleotides was quantitated by spotting dilutions of labeled probe and control dig-labeled λ phage DNA on nitrocellulose paper followed by detection with AP-labeled, anti-digoxigenin F(ab) fragments. Bound AP activity was visualized using 0.33 and 0.165 mg/ml, respectively, of nitroblue tetrazolium and 5-bromo-4-chloro-indoyl phosphate in 0.1 M Tris-HCl, pH 9.5, containing 100 mM NaCl and 50 mM $MgCl_2$, according to the manufacturer's instructions. Specificity of the probes was determined in Northern analyses of the hybridomas B1-8 (V186.2, λ_1) and TEPC-15 (V1, κ) (data not shown).

In Situ Hybridization on Frozen Sections. All steps leading to in situ hybridizations were carried out in a ribonuclease-free environment; glassware and microtome knives were baked and solutions prepared with diethylpyrocarbonate-treated double-distilled, sterile water. 6-μm-thick longitudinal spleen sections were thaw mounted onto slides coated with Denhart's solution (0.1% Ficoll, 0.1% polyvinylpyrrolidone, 0.1% BSA), air dried for 10 min, fixed in cold 4% paraformaldehyde (Sigma Chemical Co.) in PBS for 5 min, rinsed in water, and stored in 70% ethanol at 4°C until use. Spleen sections were pretreated as follows. Briefly, slides were placed in water for 5 min, 0.2 N HCl for 20 min, washed in water, permeabilized with proteinase K (Boehringer Mannheim Biochemicals) (10 μg/ml in 10 mM Tris-HCl containing 2 mM $CaCl_2$, pH 7.4) for 15 min at 37°C, post-fixed in 4% paraformaldehyde for 5 min, rinsed twice in water, acetylated by incubation (10 min, 25°C) in 0.1 M triethanolamine-HCL buffer, pH 8.0, containing 0.25% (vol/vol) acetic anhydride, washed in 2× SSC, soaked in 0.1 M Tris, 0.1 M glycine, pH 7.0, for 30 min (25°C), washed twice in 2× SSC, dehydrated via 1-min incubations in graded ethanols (70%, 80%, 90%, 100%), and air dried. Sections were then prehybridized (42°C) in a moist chamber with a prehybridization mixture composed of 50% de-ionized formamide, 4× SSC, 100 mM sodium phosphate buffer, pH 6.5, 1% SDS, and denatured salmon sperm DNA (10 μg/ml). After incubation for 6 h, this mixture was removed, and 100 μl of hybridization solution (50% de-ionized formamide, 4× SSC, 50 mM sodium phosphate buffer, pH 6.5, 1% SDS, dextran sulphate, and 20 pg/μl heat-denatured, digoxigenin-labeled probe) was applied per slide. Slides were then covered with siliconized cover slips, their edges sealed with rubber cement to minimize evaporation, and incubated at 70°C for 10 min (to remove secondary structure of the mRNA) and at 42°C for 48 h in a moist environment. Post-hybridization washes were as follows: 2× SSC containing 40% formamide at 42°C for 20 min, 1× SSC at room temperature for 60 min, and 0.1× SSC at 42°C for 30 min. Hybridized dig-labeled probe was visualized using AP-conjugated anti-digoxigenin antibody followed by enzymatic detection with NBT.BCIP as described above. Levamisole (2 mM) was added to the substrate to inhibit endogenous AP activity.

Results

λ^+ Splenocytes Are Infrequent in the Spleens of Normal or Carrier-immunized Mice. Spleens taken from normal control or CG-immunized mice do not contain large numbers of splenocytes expressing detectable levels of cytoplasmic λ L chain. Fig. 1 illustrates that λ^+ splenocytes in carrier (CG)-immunized mice are relatively rare (Fig. 1, *a* and *b*), while splenocytes expressing cytoplasmic λ L chain are abundant after immunization with NP-CG (Fig. 1 *c*). The low frequency of λ^+ cells in CG-primed animals was not due to a failure to respond, as large clusters of κ^+, CG-binding lymphocytes could be observed after incubation with enzyme conjugates of CG (Fig. 1 *a*) or goat antibody specific for mouse κ L chain (data not shown).

Appearance of λ^+, NIP-binding Cells after Administration of NP-CG. Every 2 d (days 2–16) after intraperitoneal injection of NP-CG, cohorts of mice were killed and their spleens frozen in preparation for microscopic examination; B and T lymphocyte populations were subsequently identified by reaction with fluorochrome- or enzyme-labeled antigens and antibodies.

As early as 2 d after immunization with NP-CG, low numbers of B cells containing detectable amounts of cytoplasmic λ L chain could be observed at the periphery of the PALS and around the terminal branches of the central arterioles. These loose collections of cells are generally composed of 8–16 λ^+ cells in close proximity to a splenic arteriole and are interspersed among abundant ($CD4^+$) T cells (data not shown). About 50% of these λ^+ cells bind NIP-BSA and express the Ac38 and Ac146 idiotopes.

4 d after immunization, the number of λ^+ cells within the PALS increases such that slightly more than half of the cell clusters contain ~25 (17–64) cells. While some consolidation may occur, λ^+ splenocytes remain loosely associated and intermingled with Thy-1.2^+ lymphocytes. These λ^+ cells do not bind the lectin, PNA (PNA^-).

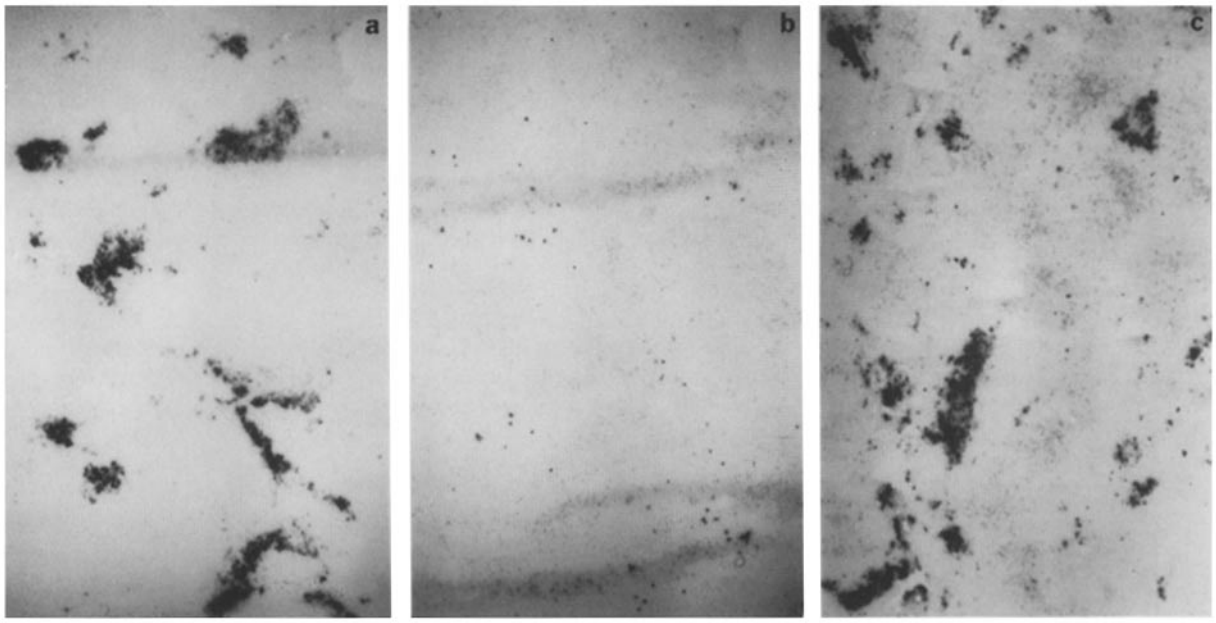

Figure 1. λ^+ foci are induced by immunization with NP-CG but not CG alone. Spleens were taken from mice immunized 8 d earlier with 50 μg CG (*a* and *b*) or NP-CG (*c*); sections of frozen spleen were labeled with CG-biotin or anti-λ-biotin followed by S-AP. Bound AP activity was visualized with NBT.BCIP. Carrier-immunized mice demonstrate a good response to CG (*a*) that uses few λ^+ B cells (*b*). In contrast, mice immunized with NP-CG produce large λ^+ foci (*c*). (*a–c*, ×40).

By day 6 post-immunization, the loosely organized clusters of NP-induced B lymphocytes condense to form foci that may contain 50–100 λ^+, PNA^- cells within a section. T cells are no longer interspersed among the responding B lymphocytes; instead, foci of λ^+ cells are invariably apposed along one face of the T cell–rich PALS (Fig. 2), extending transversally through the spleen for considerable distances. This expansion and consolidation continues, peaking at day 8 of the response. By this time, foci are essentially devoid of splenocytes that do not express cytoplasmic λ L chain and bind NIP (Fig. 3, *a* and *b*).

The processes of cellular proliferation and consolidation are reversed after day 8 post-immunization such that foci become smaller and more disperse by days 10–12. As the cells become increasingly disperse, their intimate association with the PALS is also lost. By day 12, the majority of λ^+, PNA^- cells exist as loosely organized clusters of 17–64 cells (Fig. 4).

On day 8 of the response, the formation of λ^+, PNA^+ GC is first observed. GC persist in the spleen at least until day 16 and thus coexist with well-formed λ^+, PNA^- foci for several days. Initially, GC consist of tight collections of some 20–40 cells that bind relatively low amounts of PNA.

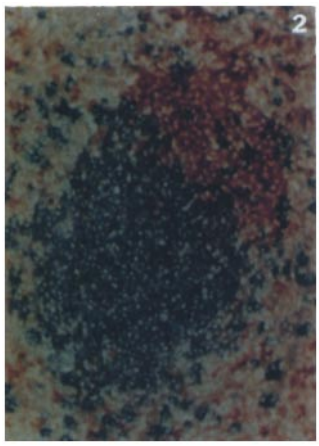

Figure 2. By day 6 of the anti-NP response, λ^+ foci condense and grow in apposition to the T cell–rich PALS. Section from a spleen taken 6 d post-immunization reveals λ^+ B cells (stained red) growing in apposition to Thy-1.2$^+$ T cells (stained blue). Section was labeled by incubation with anti-λ-HRP and anti-Thy-1.2-biotin in tandem, followed by S-AP. Bound HRP activity was visualized with 3-AEC and AP with Fast blue BB salt (×200).

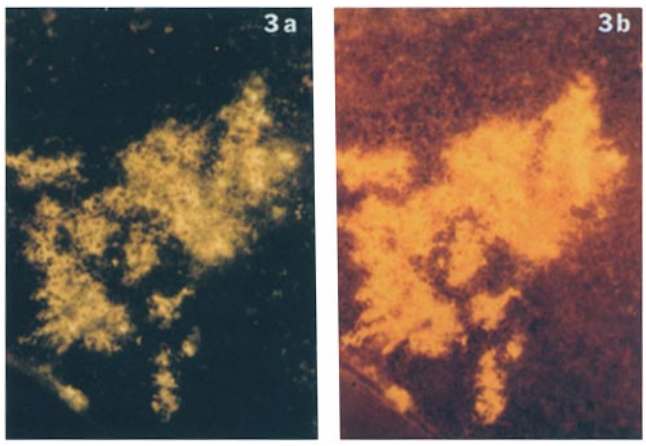

Figure 3. B cell foci reach their maximum size 8 d after immunization. A representative day 8 focus stained with anti-λ-FITC (*a*) and NIP-BSA-PE (*b*) demonstrates that by day 8 of the immune response, virtually all λ^+ B cells in the foci express the heteroclitic paratope capable of binding NIP (×200).

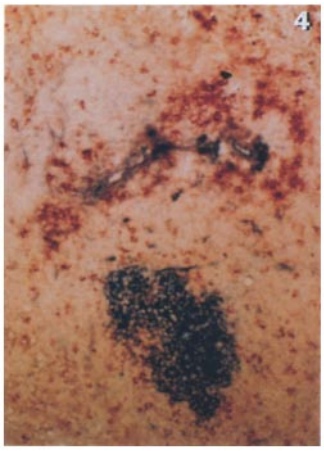

Figure 4. By day 12 of the response, B cell foci have begun their dissolution; the end of the focus-dominated response marks the initiation of GC formation. Shown is a representative photomicrograph of a splenic section illustrating day 12 after NP-CG. λ^+, PNA^- foci (stained red) have become less condensed and contain fewer cells/section. Nearby, a PNA^+ GC (stained blue) has formed. Section was labeled with anti-λ-HRP and PNA-biotin followed by S-AP. HRP and AP activities were visualized as described in Fig. 2 (×100).

By day 10, however, sectioned GC stain brilliantly with PNA and increase in size to contain 50–100 cells per section. GC reach their maximum size by day 12 and persist relatively unchanged until day 16 post-immunization. The kinetics of focus and GC growth are shown in Fig. 5.

λ^+ Foci and Germinal Centers Are Oligoclonal. To estimate the numbers of precursor cells that give rise to individual NIP-binding foci, (C57BL/6 × BALB/c)F_1 mice ($Igh^{b/a}$) were immunized with NP-CG and the numbers of NIP-binding foci that expressed the λ L chain (Igh^b-associated), bound the mAb RS-3.1 (anti-IgM^a), or both were determined by fluorescence microscopy at days 2, 4, and 6 post-immmunization. The results of this analysis are presented in Table 1. From a total of 54 foci analyzed, an average of 28% were found to express λ only, 28% bound RS-3.1 alone, and 44% were positive for both λ and IgM^a (Table 1). The expression $n = \log p/\log i$ may be used to estimate precursor frequency under these conditions (42); where i is the frequency of Igh^a or Igh^b lymphocytes, p is the proportion of pure foci (λ or IgM^a), and n is the estimated number of founding

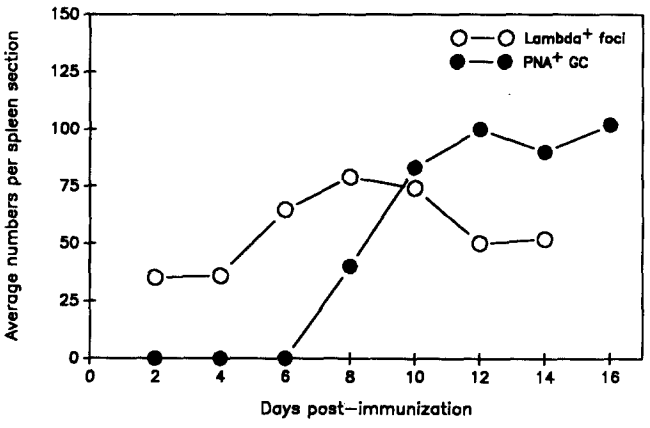

Figure 5. Kinetics of λ^+ foci and germinal center growth in spleens of immunized mice. Foci and germinal centers were identified by reactivity to fluorochrome- or enzyme-labeled anti-λ antibody or PNA and by anatomical location. Vertical axis represents the average number of foci or GC/section plotted against the time (*d*) post-immunization.

Table 1. *Frequencies of PALS-associated, NIP-binding Foci Originating from Igh^a, Igh^b, or Both Precursor Cells*

Days after immunization	Focus phenotype		
	Igh^b ($\lambda1^+$)*	Mixed ($\lambda1/IgM^{a+}$)	Igh^a (IgM^{a+})‡
		%	
2	22	50	28
4	23	45	32
6	43	36	21
	28§	44§	28§

Spleen sections from immunized (C57BL/6 × BALB/c)F_1 mice were double stained with RS 3.1-FITC and Ls136-PE.
* Detected by the antibody Ls136-PE.
‡ Detected by the antibody RS3.1-FITC.
§ Weighted averages.

precursor cells. Assuming that in the F_1 mouse $i = 0.5$, and solving for n, we estimate that each focus is derived from one to three precursor B cells. In general, frequencies determined for earlier foci (days 2 and 4) indicate precursor numbers at the upper end of this range, while estimates made at day 6 are consistent with slightly fewer precursors (Table 1).

We generated estimates of the number of founding precursors for individual GC based upon antigen specificity. Adjacent sections through GC were incubated with enzyme-labeled Ls136 and CG (AP and HRP, respectively) to determine the numbers of GC expressing λ_1, binding CG, or both. Using the same expression used for foci, we estimate that GC are also founded by one to three B cells (Table 2). This result is identical to that observed earlier in rats (42).

λ^+ Foci and Germinal Centers Are Discrete. Collections of serial sections through approximately one-half of the splenic depth were stained in tandem with anti-Thy-1.2-AP and anti-λ-HRP. Composite photographs of each section were assembled and transformed into x, y, and z coordinates using a digitizing tablet and the three-dimensional reconstruction program, PC3D. Reconstructions were made for spleens at 8 and 12 d post-immunization in order follow both foci and GC. Fig. 6 illustrates the distribution of 51 λ^+ foci within a single spleen 8 d after challenge. Note that while foci may have complex shapes and extend transversely for considerable distances, each focus is anatomically distinct. Adjacent foci are most often separated by the PALS, and extend for their entire length in intimate contact with these T cell–rich areas. Of the 51 foci seen, 38 (75%) were wholly contained within the sectioned region of the spleen and were determined to have an average volume of $5.7(\pm4.9) \times 10^5\ \mu M^3$ (range = $0.7–23.7 \times 10^5\ \mu m^3$). Together, all foci within this series of sections comprised ~0.9% of the relevant splenic volume, suggesting that at the apex of the primary response to NP-CG, no more than 1% of splenocytes participate by increased Ig synthesis.

Table 2. *Frequencies of Mixed (λ^+ and CG^+) and Pure (λ^+ or CG^+) Foci and Germinal Centers*

Days after immunization	Foci		Germinal centers	
	Mixed (λ^+ & CG^+)	Pure (λ^+ or CG^+)	Mixed (λ^+ & CG^+)	Pure (λ^+ or CG^+)
	%		%	
6	55	45	ND	ND
8	62	38	ND	ND
10	ND	ND	63	37
12	ND	ND	79	21
14	ND	ND	68	32
16	ND	ND	65	35

Spleen sections from immunized C56BL/6 mice (days 6–16) were double stained with anti-λ-FITC and CG-PE. Individual foci and GC were scored for λ or CG binding, and frequencies of mixed (λ^+ foci/GC containing CG^+ cells) and pure (λ^+ or CG^+ only) foci and GC are tabulated.

Reconstructions of GC were also obtained, and Fig. 7 illustrates a splenic volume containing 52 PNA^+ GC 12 d post-immunization. 15 GC are contained wholly within the serial sections and comprise a total volume of 98.5×10^5 μm^3. We estimate that some 300–500 GC are present within the entire spleen 12 d after immunization; ~55% of GC contain λ^+, NIP-binding cells, the remainder are specific for CG (23%) or are of unknown specificity (22%).

Upper limits for the number of B cells participating in the anti-NP response may be calculated from the average volume, numbers of foci and GC, and the proportion that bind NIP. Assuming an average cell diameter of 10 μm for these for activated cells, no more than $\sim 2.5 \times 10^5$ cells can be present in foci or GC at a single point in time. Analogous calculations may be used to estimate average division rates based upon the independence and oligoclonal nature of foci and GC. Estimates for division times range from 16–20 h for foci to 12–14 h for GC with the assumption that on average, two precursor cells initiate both structures.

Isotype Switch in Foci and GC. To determine the onset and extent of class switch in foci and GC during the response, λ^+ cells were counter labeled with anti–mouse IgG-PE. The kinetics of the appearance of double-positive B cells (λ^+, IgG^+) in foci is illustrated in Fig. 8. Among all λ^+ cells, only 20–25% label with anti-IgG on days 2–6 post-immunization. At these times, all IgG^+ cells were interspersed with a majority of IgG^- cells, no pure IgG^+ foci were observed. By day 8, the numbers of IgG^+, λ^+ cells increased substantially, and for the first time, pure IgG^+ foci were observed. The numbers of λ^+, IgG^+ cells in foci in-

Figure 6. Reconstruction of d8 λ^+ foci demonstrating that each focus is a discrete structure. 70 (6-μm) serial sections were cut from an immune spleen; every fifth section was stained with anti-λ-HRP and anti-Thy-1.2-AP. Bound enzymatic activity was visualized as for Fig. 3. The entire spleen was photographed in overlapping series (×40), and montages were assembled. All λ^+ foci and Thy-1.2$^+$ regions in one-half of each section were given digital coordinates using the PC3D software and a digitizing tablet (Jandel). The computer-generated reconstruction demonstrates the extensive transverse growth of λ^+ foci as well as their independence. Individual foci have been assigned colors to aid visualization. For clarity, Thy-1.2$^+$ regions are not shown.

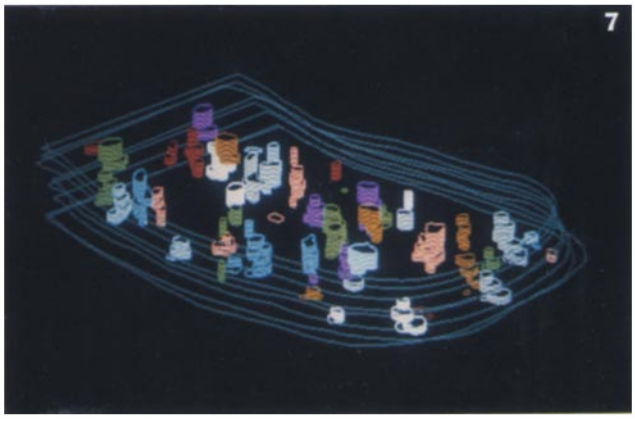

Figure 7. Three-dimensional reconstruction of a single spleen depicting PNA^+ day 12 germinal centers. 35 serial frozen sections were cut from spleen of a mouse challenged with 50 μg NP-CG/alum 12 d earlier. Every fifth section was stained with PNA-AP followed by NBT.BCIP, and three-dimensional reconstruction was made as described in Fig. 6. Individual germinal centers were assigned colors for clarity.

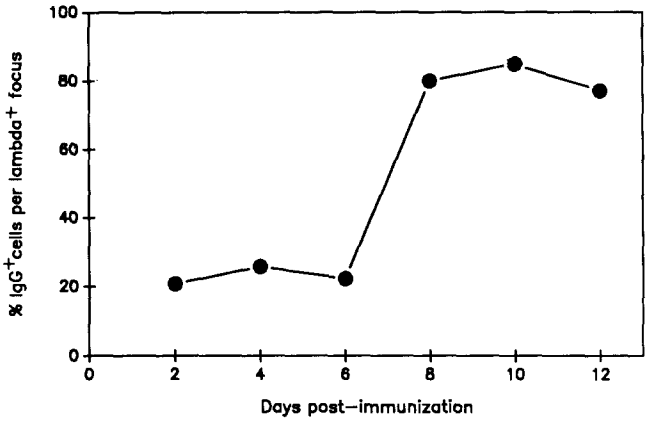

Figure 8. Kinetics of IgM → IgG switching in λ⁺ foci. Spleen sections (day 2–12) were tandemly stained with anti-λ-FITC and anti-IgG-PE, and the frequency of IgG⁺, λ⁺ B cells within λ⁺ foci was determined by scoring λ⁺, IgG⁺ (green/red) and λ⁺, IgG⁻ (green only) cells. Data are represented as the mean frequency of IgG⁺ cells/λ⁺ focus at days 2–12 post-immunization.

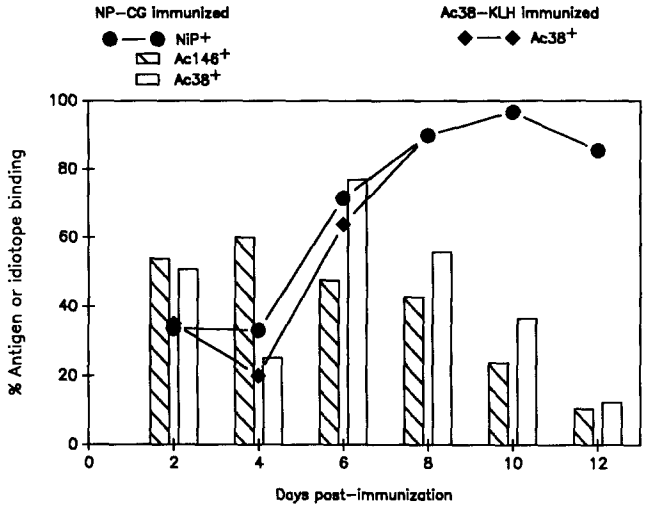

Figure 9. Kinetics of heteroclitic antigen binding and expression of idiotopes within individual λ⁺ foci of mice immunized with 50 μg of either NP-CG or Ac38-KLH. Serial sections (day 2–12) from immunized mice were double stained with anti-λ-FITC and NIP-BSA-PE, Ac38-PE, or Ac146-PE. The frequency of cells (within single λ⁺ foci) binding NIP and expressing idiotopes was ascertained by analyzing adjacent serial sections. Similarly, sections (days 2–8) from mice immunized with Ac38-KLH were stained with anti-λ-FITC and Ac38-PE, and the frequency of λ⁺, Ac38⁺ (green/red) and λ⁺, Ac38⁻ (green only) focus cells was determined. λ⁻, Ac38⁺ foci were excluded from analysis. The vertical axis depicts the average frequencies of B cells expressing NIP, Ac38, and Ac146 binding/λ⁺ focus, and the horizontal axis denotes days post-immunization. A total of 506 λ⁺ foci from 16 NP-CG immunized mice were analyzed, and for Ac38-KLH immunized mice, a total of 40 λ⁺ foci from four mice were studied.

creased little more on days 10–12, plateauing at ~85%. About 40% of all d10 λ⁺ foci were made up of only IgG⁺ cells. Interestingly, the switch from IgM to IgG expression occurred within a relatively short period of time (Fig. 8) and showed no correlation with focus size (data not shown). These findings suggest that some systemic activity may catalyze class switch in vivo. All germinal centers were almost exclusively IgG⁺.

Antigen-dependent Phenotypic Changes in PALS-associated Foci. Composite phenotypes for individual foci were ascertained by reacting adjacent serial sections with anti-λ-FITC in pairwise combination with NIP-PE, Ac38-PE, and Ac146-PE. In this way, λ⁺ cells from foci obtained 2–12 d after immunization could be scored for the heteroclitic antigen binding and expression of idiotopes thought to be hallmarks of the primary anti-NP response (24–27).

Determination of composite phenotypes expressed by single foci clearly demonstrated the individuality of these populations. Even neighboring foci frequently contained very different proportions of cells expressing heteroclitic specificity or the

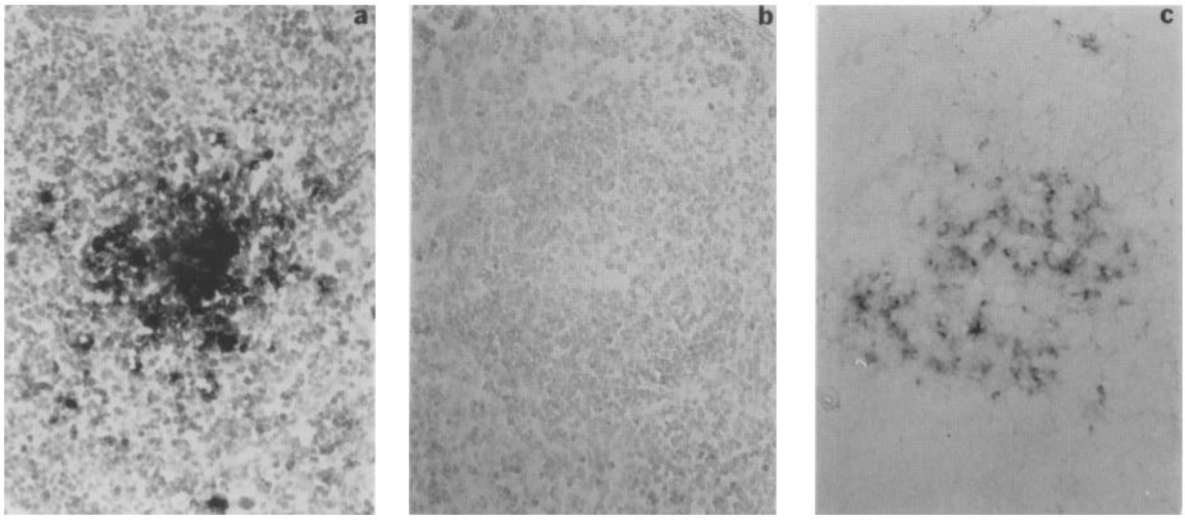

Figure 10. λ⁺ B cell foci that did not express the Ac38 or Ac146 idiotopes utilized V region gene segments complementary to V186.2 and λ_1 DNA gene probes. Three serial sections of a spleen recovered 8 d after immunization with NP-CG have been labeled with (*a*) Ls136-biotin, (*b*) Ac38-biotin, and (*c*) a dig-labeled V186.2 gene probe. Hybridized dig was identified with anti-dig antibody coupled to AP. Bound biotin was reacted with S-AP. AP activity was visualized with NBT.BCIP. The illustrated λ⁺ focus (*a*) bound NIP (data not shown), but was entirely negative for the Ac38 idiotope (*b*). However, cells within the focus specifically hybridized with a V186.2 probe (*c*) and a λ_1 probe (data not shown). (*a–c*, ×200).

idiotopes Ac38 and Ac146. Further, these markers appeared to be essentially independent, the presence or absence of any marker did not influence the expression of the others (data not shown). These findings are compatible with our observations that foci represent anatomically distinct oligoclonal populations, and with the observations of Bruggemann et al. (39) on the molecular structure of anti-NP antibodies.

In spite of the variability of phenotypes expressed among individual foci within a spleen, a general pattern of NIP binding and idiotope expression within foci emerged over the course of the response (Fig. 9). At days 2 and 4 post-immunization, some 35–55% of λ^+ cells within foci exhibit heteroclitic antigen binding (NIP^+) and express the Ac38 and Ac146 idiotopes. These frequencies increase in unison by day 6 to 60–70%; thereafter, the patterns of NIP binding and idiotope expression diverge. From days 6 until day 12, the frequency of $Ac38^+$ and $Ac146^+$ cells declines monotonically, while the frequency of heteroclitic B cells (NIP^+) increases to ~90% (Fig. 9).

The divergence in patterns of paratopic and idiotopic expression suggested that the phenotypic changes we observed might represent paratopic selection by antigen. Presumably, expression of the heteroclitic combining site underwent positive selection during the response, while idiotope expression was either neutral or selected against. To test this hypothesis, we injected mice with Ac38-KLH, an immunogenic conjugate known to elicit substantial amounts of λ^+, $Ac38^+$ antibody (35). In these mice, Ac38 expression is analogous to NIP binding in NP-immunized mice (35); significantly, the dynamics of Ac38 expression within λ^+ foci induced by Ac38-KLH almost exactly mirrors that of NIP-binding cells in mice immunized with NP-CG (Fig. 9).

Phenotypes of λ^+ GC Cells. Determinations analogous to those used to characterize the paratopic and idiotopic phenotypes of λ^+ cells within PALS-associated foci were used in an attempt to define the phenotype of GC cells. Adjacent serial sections of day 12 spleen were reacted with anti-λ-FITC paired with PNA-PE, NIP-PE, Ac38-PE, and Ac146-PE. However, the relatively low levels of cytoplasmic Ig in GC B cells resulted in only a faint staining that made the determination of complex phenotypes for individual cells problematic. Nonetheless, a large majority of λ^+, PNA^+ GC exhibited diffuse staining with labeled antiidiotope and NIP.

In Situ Hybridization of Splenic Foci and GC. Changes observed in the paratopic and idiotopic phenotype of antigen-induced foci could reflect the growth of clones expressing V region gene segments other than the expected V186.2/$V_\lambda 1$ combination (28). Therefore, we hybridized sections of spleen taken 4 and 12 d after immunization with DNA probes complementary to V186.2 and λ1. Adjacent serial sections were labeled with AP-labeled Ac38, NIP, or anti-λ antibody. Among >120 λ^+ foci analyzed, all, including those that did not express the Ac38 idiotope or heteroclitic antigen-binding, hybridized with both V region probes (Fig. 10). In contrast, only ~35% of the few λ^+ foci generated by immunization with CG alone (Fig. 1) hybridized the V186.2 probe (data not shown). This frequency is in the range of that expected for stochastic expression of the J558 V_H gene family, of which V186.2 is a member (2–5).

As might be expected from the lower levels of cytoplasmic Ig within GC, hybridization to GC was more faint than achieved with foci, however, >70% of all λ^+ GC were labeled by the V186.2 and λ_1 probes (data not shown).

Isotype Switch and Phenotypic Variability of Foci and GC. No correlation between phenotypic change and IgM → IgG class switch was observed for foci and GC. By the time (day 8–10) large numbers of λ^+ cells began to express IgG, most of the patterned shifts in the paratopic and idiotopic phenotypes of focus cells had already taken place (compare Figs. 8 and 9). GC cells are almost exclusively IgG^+, and it was not possible to determine complex phenotypes for individual cells with certainty. However, most λ^+ GC contained numbers of cells that expressed the Ac38 and Ac146 idiotopes and bound NIP (see above).

Discussion

We have used reagents specific for phenotypic and genotypic hallmarks of the anti-NP response (24–28) to detail the architecture and clonal dynamics of a well-studied immune response. While this approach is not novel (38, 43–46), the combination of techniques used has permitted us to detail for the first time the natural history of an immune response in vivo.

The splenic white pulp is organized about central arterioles that are coaxially surrounded by the T cell–rich PALS. In turn, these structures are encompassed by the B lymphocytes, macrophages, and dendritic cells of the lymphoid follicle (reviewed in references 47 and 48). It is within the white pulp, in the periphery of the PALS and near terminal branches of the central arteriole, that λ^+ B cells are first observed after immunization. This is in agreement with earlier histological studies (reviewed in reference 45). By day 8 of the response, continued proliferation of these antigen-activated cells generates large oligoclonal foci of B lymphocytes (Fig. 3). Thereafter, these PNA^- foci decrease in size, becoming rare or absent by day 14–16 (Fig. 4). A second, anatomically distinct population of PNA^+ B cells form GC on day 8–10 that reach their maximum size by day 12. The great majority of GC persist at least until day 16 post-immunization.

Based upon computer-aided reconstructions of serially sectioned splenic tissue, we estimate that no more than 100–150 foci and 300–500 GC are present in the spleen during the height of the primary response to NP (Figs. 6 and 7). Approximately 95% of λ^+ foci bind the hapten NIP, while ~55% of PNA^+ GC do so. Both foci and GC achieve maximum volumes of $6–7 \times 10^5\ \mu m^3$, accounting for as much as 1% of the total splenic volume. Based upon three-dimensional volume measurements of individual foci and germinal centers, and assuming an average cell diameter of 10 μm, we estimate the division times for B cells in foci and GC to be 16–20 and 12–14 h, respectively. Although these values do not consider cell death or emigration, they are in good agreement with those reported in the literature (49, 50).

Isotype switching in foci, from IgM to IgG, occurred within

a short period of time (days 6–8) (Fig. 8). Interestingly, class switch frequencies did not depend upon focus size or anatomical location within the spleen; foci of all sizes switched from IgM expression to IgG in concert, within a matter of 48 h. This finding suggests that in vivo some systemic activity, presumably a lymphokine(s), may activate the switch-recombinase to catalyze a generalized isotype switch.

Individual foci and GC were found to be oligoclonal (Tables 1 and 2). Despite considerable variability among the composite phenotypes of individual foci, in general, the frequency of λ^+ cells that did not express the Ac38 and Ac146 idiotopes increased over time while the proportion of non-heteroclitic B cells (NIP^-) declined (Fig. 9). This pattern of idiotype loss was reversed in mice immunized with Ac38-KLH, implying that these population changes are driven by antigen (Fig. 9).

Population changes within foci could reflect at least two distinct processes. First, they may be only apparent, the product of binding artifacts. This is especially likely during the early days of the response, when levels of induced cytoplasmic Ig may be relatively low. Hapten binding might prove especially sensitive to this problem due to the relatively low affinity of primary anti-NP antibody (36, 51); binding of the antiidiotopes Ac38 and Ac146 should be less affected by lower amounts of cytoplasmic Ig, however, due to their relatively high affinities (27, 51). Significantly, only B cells containing sufficent λ^+ cytoplasmic Ig to be detected by the mAb, Ls136, were studied; this antibody, specific for the λ_1 L chain, has an affinity for the B1-8 hybridoma protein (IgM, λ_1; $Ac38^+$) almost exactly equal to that of antibody Ac38 (27). Second, these changes may represent competition among oligoclonal populations of genetically dissimilar B cells for limiting amounts of antigen. Initially, a small number of NP-specific B cells initiate individual foci (Table 1); with time, the relative proportions of the founding clones may change in response to selective growth advantages conferred by the (paratopic) phenotype. As all λ^+ foci studied hybridized V region probes complementary to the expected V_H and V_λ gene segments (Fig. 10), it seems likely that the genetic basis for the observed phenotypic diversity resides in alternative D/J_H associations, the effects of junctional or N sequence diversity, and/or somatic mutation.

Although most studies have found that somatic hypermutation does not occur before day 7–10 of the primary response (30–34), recent findings by Levy et al. (52) suggest that mutation may begin as early as 2 d after immunization. Our own work suggests that somatic mutation does not occur at significant rates in foci while the mutation frequency in GC is on the order of 10^{-3}/bp/division (unpublished results). This leads us to believe that the most likely explanation for changes in the phenotype of focus B cell populations is affinity-based competition among unmutated cells. Presumably, then, in mice immunized with NP-CG, expression of the heteroclitic paratope is favored, while Ac38 and Ac146 idiotope expression is either selectively neutral or negative. The dominant focus phenotype at day 8 (λ^+; $Ac38^-$; $Ac146^-$; NIP^+) may then represent the optimum anti-NP germline phenotype that can be efficiently generated by the C57BL/6 mouse.

A second distinct population of antigen-activated B cells is observed on day 8–10 of the primary response with the formation of some 300–500 PNA^+ GC. Of these, ~55% or ~220 were λ^+. Thus, there is a rough correspondence between the numbers of λ^+ foci (100–150) and GC within the spleen. Lower levels of cytoplasmic Ig within the GC B cells made it impossible to follow phenotypic changes that may take place in the GC, however ≥80% of λ^+ GC exhibited heteroclitic antigen binding and expressed the Ac146 and Ac38 idiotopes. In collaboration with U. Weiss and K. Rajewsky, we have demonstrated that GC B cell populations frequently contain the progeny of a single founder cell that constitute a single genealogy generated by a step-wise process of somatic hypermutation and selection (unpublished results). Thus, GC seem to represent sites of predominantly intraclonal competition for antigen among mutated sister cells, while foci may be examples of interclonal competition between unrelated clones expressing unmutated V region gene segments.

The relationship between cells within foci and GC remains unclear. These structures are anatomically distinct, and even though foci and GC coexist during part of the primary response, our impression from reviewing many sections is that foci do not become GC. Indeed, even during their dissolution, B cells within foci are uniformly PNA^- and express composite Ig phenotypes that seem to differ from that often found in GC. This raises the interesting possibility that the B cells within foci and GC may represent two distinct populations. On the other hand, our findings do not preclude the migration of some small number of focus B cells, perhaps those that have best competed for antigen, to the nascent GC. To resolve this question, we are in the process of determining the relatedness of adjacent foci and GC by amplifying V genes from adjacent foci and GC in order to sequence CDR3 regions from both populations.

The numbers of hapten-specific foci and GC in the spleen agree well with estimates of the number of independent lineages thought to give rise to primary antihapten responses (33, 53). Both foci and GC are anatomically isolated, the products of (apparently) independent founding events. Further, the B cell populations of individual foci and GC evolve along unique pathways in the course of the immune response. These events generate isolated pauciclonal populations of antibody-forming cells that are genetically distinct. Thus, it may not be inappropriate to consider the primary antibody response as the product of some 100–200 or so independent "islands" of antigen-reactive cells.

This analogy raises interesting questions about the population genetics of lymphocytes responding to antigen. For example, as there seems to be little or no gene flow between individual foci and GC, affinity-based competition for antigen must only occur within these structures and not between them. This should lead to hundreds of local affinity-selected populations. Interestingly, such diversity is not observed in the secondary response (54–56), suggesting that some further mechanism operates to reduce the number of clones destined to participate in memory responses.

We thank Drs. T. Imanishi-Kari, A. L. M. Bothwell, and K. Rajewsky for the gifts of reagents, and Dr. J. Cerny for the GK1.5 cell line and informative discussions on splenic histology. Ms. Jacqueline Fields provided excellent secretarial assistance.

This work was supported by U.S. Public Health Service grants AI-24335 and AG-08182.

Address correspondence to Garnett Kelsoe, Department of Microbiology and Immunology, University of Maryland School of Medicine, 655 W. Baltimore St., Baltimore, MD 21201.

Received for publication 6 December 1990 and in revised form 6 February 1991.

References

1. Dildrop, R., U. Krawinkel, E. Winter, and K. Rajewsky. 1985. V_H-gene expression in murine lipopolysaccharide blasts distributes over the nine known V_H-gene groups and may be random. *Eur. J. Immunol.* 15:1154.
2. Schulze, D.H., and G. Kelsoe. 1987. Genotypic analysis of B cells by in situ hybridization: stoichiometric expression of three V_H families in adult C57BL/6 and BALB/c mice. *J. Exp. Med.* 166:163.
3. Jeong, H.D., J.L. Komisar, E. Kraig, and J.M. Teale. 1988. Strain-dependent expression of V_H gene families. *J. Immunol.* 140:2436.
4. Kelsoe, G., R. Miceli, J. Cerny, and D.H. Schulze. 1989. Mapping of antibody specificities to V_H gene families. *Immunogenetics.* 29:288.
5. Sheehan, K.M., and P.H. Brodeur. 1989. Molecular cloning of the primary *IgH* repertoire: a quantitative analysis of V_H gene usage in adult mice. *EMBO (Eur. Mol. Biol. Organ.) J.* 8:2313.
6. Kaushik, A., D.H. Schulze, C.A. Bona, and G. Kelsoe. 1989. Murine Vκ gene expression does not follow the V_H paradigm. *J. Exp. Med.* 169:1859.
7. Teale, J.M., and Morris, E.G. 1989. Comparison of V_κ gene family expression in adult and fetal B cells. *J. Immunol.* 143:2768.
8. Lawler, A.M., J.F. Kearney, M. Kuehl, and P. Gearhart. 1989. Early rearrangements of genes encoding murine immunoglobulin κ chains, unlike genes encoding heavy chains, use variable gene segments dispersed throughout the locus. *Proc. Natl. Acad. Sci. USA.* 86:6744.
9. Kalled, S.L., and P.H. Brodeur. 1990. Preferential rearrangement of $V_\kappa 4$ gene segments in pre-B cell lines. *J. Exp. Med.* 172:559.
10. Tonegawa, S. 1983. Somatic generation of antibody diversity. *Nature (Lond.).* 286:676.
11. Desiderio, S.V., G.D. Yancopoulos, M. Paskind, E. Thomas, M.A. Boss, N. Landau, F.W. Alt, and D. Baltimore. 1984. Insertion of *N* regions into heavy chain genes is correlated with expression of terminal deoxytransferase in B cells. *Nature (Lond.).* 311:752.
12. Feeney, A.M. 1990. Lack of *N* regions in fetal and neonatal mouse immunoglobulin V-D-J junctional sequences. *J. Exp. Med.* 172:1377.
13. Kaushik, A., D.H. Schulze, F.A. Bonilla, C.A. Bona, and G. Kelsoe. Stochastic pairing of heavy-chain and κ light-chain variable gene families occurs in polyclonally activated B cells. *Proc. Natl. Acad. Sci. USA.* 87:4932.
14. Kelsoe, G., and D. Farina. 1987. Is the antibody repertoire biased? *In* Evolution and Vertebrate Immunity. G. Kelsoe and D.H. Schulze, editors. University of Texas Press, Austin, TX. 163–174.
15. White-Scharf, M.E., M. Souroujon, J. Andre-Schwartz, R.S. Schwartz, and M.L. Gefter. 1988. Specificity of the germline-encoded preimmune B cell repertoire. *In* B Cell Development. O.N. Witte, N.R. Klinman, and M.C. Howard, editors. Alan R. Liss, Inc., New York. 105–1187,
16. Striebich, C.C., R.M. Miceli, D.H. Schulze, G. Kelsoe, and J. Cerny. 1990. Antigen-binding repertoire and immunoglobulin heavy chain gene usage among B cell hybridomas from normal and autoimmune mice. *J. Immunol.* 144:1857.
17. Miller, H.R.P., T. Ternynck, and S. Avrameas. 1975. Synthesis of antibody and immunoglobulin without detectable antibody function in cells responding to horseradish peroxidase. *J. Immunol.* 114:626.
18. Antoine, J.C., and S. Avrameas. 1976. Correlation between immunoglobulin- and antibody-synthesizing cells during primary and secondary immune responses of rats immunized with HRP. *Immunology.* 30:537.
19. Nemazee, D., and V. Saito. 1983. Induction of rheumatoid antibodies in the mouse. Regulated production of autoantibody in the secondary humoral response. *J. Exp. Med.* 158:529.
20. Klinman, N.R. 1969. Antibody with homogenous antigen binding produced by splenic foci in organ culture. *Immunochemistry.* 6:757.
21. Metcalf, D., G.J.V. Nossal, N.L. Warner, J.F.A.P. Miller, T.E. Mandel, J.E. Layton, and G.A. Gutman. 1975. Growth of B lymphocyte colonies in vitro. *J. Exp. Med.* 142:1534.
22. Anderson, J., A. Coutinho, W. Lernhardt, and F. Melchers. 1977. Clonal growth and maturation to immunoglobulin secretion in vitro of growth-inducible B lymphocyte. *Cell.* 10:27.
23. Kelsoe, G. 1987. Cloning of mitogen- and antigen-reactive B lymphocytes on filter paper disks: phenotypic and genotypic analysis of B cell colonies. *Methods Enzymol.* 150:287.
24. Imanishi-Kari, T., and O. Makela. 1973. Strain differences in the fine specificity of mouse anti-hapten antibodies. *Eur. J. Immunol.* 3:323.
25. Jack, R.S., T. Imanishi-Kari, and K. Rajewsky. 1977. Idiotypic analysis of C57BL/6 mice to the (4-hydroxy-3-nitrophenyl)acetyl group. *Eur. J. Immunol.* 7:559.
26. Makela, O., and K. Karjalainen. 1977. Inherited immunoglobulin idiotypes of the mouse. *Immunol. Rev.* 34:119.
27. Reth, M., T. Imanishi-Kari, and K. Rajewsky. 1979. Analysis of the repertoire of anti-NP antibodies in C57BL/6 mice by cell fusion. II. Characterization of idiotypes by monoclonal anti-idiotype antibodies. *Eur. J. Immunol.* 9:1004.
28. Bothwell, A.L.M., M. Paskind, M. Reth, T. Imanishi-Kari,

K. Rajewsky, and D. Baltimore. 1981. Heavy chain variable region contribution to the NP^b family of antibodies: somatic mutation evident in a γ2a variable region. *Cell.* 24:625.
29. Rose, M.L., M.S.C. Birbeck, V.J. Wallis, J.A. Forrester, and A.J.S. Davies. 1980. Peanut lectin binding properties of germinal centres of mouse lymphoid tissue. *Nature (Lond.).* 284:364.
30. Clarke, S.H., K. Huppi, D. Ruezinsky, L. Staudt, W. Gerhard, and M. Weigert. 1985. Inter- and intraclonal diversity in the antibody response to influenza hemagglutinin. *J. Exp. Med.* 161:687.
31. Allen, D., A. Cumano, R. Dildrop, C. Kocks, K. Rajewsky, N. Rajewsky, J. Roes, F. Sablitzky, and M. Siekevitz. 1987. Timing, genetic requirements and functional consequences of somatic hypermutation during B-cell development. *Immunol. Rev.* 96:5.
32. Berek, C., and C. Milstein. 1987. Mutation drift and repertoire shift in the maturation of the immune response. *Immunol. Rev.* 96:23.
33. Manser, T., L.J. Wysocki, M.N. Margolies, and M.L. Gefter. 1987. Evolution of antibody variable region structure during the immune response. *Immunol. Rev.* 96:141.
34. Malipiero, U.V., N.S. Levy, and P.J. Gearhart. 1987. Somatic mutation in anti-phosphorylcholine antibodies. *Immunol. Rev.* 96:59.
35. Tesch, H., T. Takemori, and K. Rajewsky. The immune response against anti-idiotope antibodies. II. The induction of antibodies bearing the target idiotope (Ab3β) depends on the frequency of the corresponding B cells. *Eur. J. Immunol.* 13:726.
36. Reth, M., G.J. Hamerling, and K. Rajewsky. 1978. Analysis of the repertoire of anti-NP antibodies in C57BL/6 mice by cell fusion. I. Characterization of antibody families in the primary and hyperimmune response. *Eur. J. Immunol.* 8:393.
37. Schuppel, R., J. Wilke, and E. Weiler. 1987. Monoclonal anti-allotype antibody towards BALB/c IgM. Analysis of specificity and site of a V-C crossover in recombinant strain BALB-Igh-V^a/Igh-C^b. *Eur. J. Immunol.* 17:739.
38. Brown, A.R., and E. Claassen. 1988. Detection of antibody, idiotype and anti-idiotype forming cells by *in situ* immunocytochemical staining. *J. Immunol. Methods.* 109:235.
39. Bruggeman, M., H.J. Muller, C. Burger, and K. Rajewsky. 1986. Idiotype selection of an antibody mutant with changed hapten binding specificity resulting from a point mutation in position 50 of the heavy chain. *EMBO (Eur. Mol. Biol. Organ.) J.* 5:1562.
40. Bothwell, A.L.M., M. Paskind, M. Reth, T. Imanishi-Kari, K. Rajewsky, and D. Baltimore. 1982. Somatic variants of murine immunoglobulin λ light chains. *Nature (Lond.).* 298:380.
41. Maniatis, T., E.F. Fritisch, and J. Sambrook. 1982. Molecular Cloning: A Laboratory Manual. Cold Spring Harbor Laboratory, Cold Spring Harbor, NY.
42. Kroese, F.G.M., A.S. Wubbena, H.G. Seijen, and P. Nieuwenhuis. 1988. The *de novo* generation of germinal centres is an oligoclonal process. *Adv. Exp. Med. Biol.* 237:245.
43. Nieuwenhuis, P., and D. Opstelten. 1984. Functional anatomy of germinal centers. *Am. J. Anat.* 170:421.
44. Rooijen, N.V., E. Claassen, and P. Eikelenboom. 1986. Is there a single differentiation pathway for all antibody-forming cells in the spleen? *Immunol. Today.* 7:193.
45. Rooijen, N.V. 1990. Direct intrafollicular differentiation of memory cells into plasma cells. *Immunol. Today.* 11:154.
46. Delemarre, F.G.A., E. Claassen, and N.V. Rooijen. 1989. Primary *in situ* immune response in popliteal lymph nodes and spleen of mice after subcutaneous immunization with thymus-dependent or thymus-independent (Type 1 and 2) antigens. *Anat. Rec.* 223:152.
47. Weiss, L. 1964. The white pulp of the spleen. The relationship of arterial vessels, reticulum and free cells in the peripheral lymphatic sheath. *Bull. Johns Hopkins Hosp.* 115:99.
48. Witmer, M.D., and R.M. Steinman. 1984. The anatomy of peripheral lymphoid organs with emphasis on accessory cells: light microscopic immunocytochemical studies of mouse spleen, lymph node and Peyer's patch. *Am. J. Anat.* 170:465.
49. Fliedner, T.M., M. Kroese, E.P. Cronkite, and J.S. Robertson. 1964. Cell proliferation in germinal centers of rat spleen. *Ann. NY Acad. Sci.* 113:578.
50. Zaitoun, A.M. 1980. Cell population kinetics of the germinal centers of lymph nodes of BALB/c mice. *J. Anat.* 130:131.
51. Rooijen, N.V., R.V. Nieuwmegen, N. Kors, and P. Eikelenboom. 1984. The development of specific antibody-containing cells in the spleen of rabbits during the secondary immune response against free or liposome associated albumin antigen. *Anat. Rec.* 208:579.
52. Levy, N.S., U.V. Malipiero, S.G. Lebecque, and P.J. Gearhart. 1989. Early onset of somatic mutation in immunoglobulin V_H genes during the primary immune response. *J. Exp. Med.* 169:2007.
53. Tao, W., and A.L.M. Bothwell. 1990. Development of B cell lineages during a primary anti-hapten immune response. *J. Immunol.* 145:3216.
54. Cumano, A., and K. Rajewsky. 1986. Clonal recruitment and somatic mutation in the generation of immunologic memory to the hapten NP. *EMBO (Eur. Mol. Biol. Organ.) J.* 5:2459.
55. Blier, P.R., and A.L.M. Bothwell. 1987. A limited number of B cells lineages generates the heterogeneity of a secondary immune response. *J. Immunol.* 139:3996.
56. Allen, D., T. Simon, F. Sablitzky, K. Rajewsky, and A. Cumano. 1988. Antibody engineering for the analysis of affinity maturation on an anti-hapten response. *EMBO (Eur. Mol. Biol. Organ.) J.* 7:1995.